Cholesteric-Azobenzene Liquid Crystalline Copolymers: Design, Structure and Thermally Responsive Optical Properties

Journal:	*Polymer Chemistry*
Manuscript ID	PY-ART-04-2019-000536.R1
Article Type:	Paper
Date Submitted by the Author:	31-May-2019
Complete List of Authors:	Ndaya, Dennis; University of Connecticut, Storrs, Department of Chemistry and Polymer Program, IMS Bosire, Reuben; University of Connecticut, Storrs, Department of Chemistry Kasi, Rajeswari; University of Connecticut, Storrs, Chemistry and Polymer Program, IMS

CHOLESTERIC-AZOBENZENE LIQUID CRYSTALLINE COPOLYMERS: DESIGN, STRUCTURE AND THERMALLY RESPONSIVE OPTICAL PROPERTIES.

Dennis Ndaya[†], Reuben Bosire[†], Rajeswari M. Kasi[†,§] *

[†]Department of Chemistry, University of Connecticut, Storrs, CT 06269 (USA)

[§]Polymer Program, Institute of Material Science, University of Connecticut, Storrs, CT 06269 (USA)

Abstract.

We report synthesis of new functional cholesteric-azobenzene side-chain liquid crystalline copolymers and terpolymers, their temperature-responsive mesophase behavior, and stimuli responsive photonic properties from 400 nm to the near infra-red region of the electromagnetic spectra. Polynorbornene copolymers are synthesized using norbornene based n-alkyloxy cholesteryl (NBCh9) and norbornene based n-alkyloxy azobenzene moiety bearing different terminal functional groups (NBAz12-X, X=H, CN, CH_3O, and NO_2) by ring opening metathesis polymerization with modified second-generation Grubbs catalyst. Polynorbornene terpolymers of NBCh9, NBAz12-X, and norbornene bearing poly (ethylene glycol) (NBMPEG) are synthesized in a similar way.

The copolymers and terpolymers self-assemble to form cholesteric mesophases (N*) primarily from cholesterol molecules which forms the major phase and within which (1) azobenzene moieties serve as a molecular switch to tune the helical pitch of the cholesteric mesophase leading to wavelength modulation from the visible to near infrared range and (2) PEG provides internal plasticizing ability and mechanical integrity for easy processing of free-standing films. Unlike other azo based homopolymers and azo/cholesterol-based copolymers, this new copolymer and terpolymer platform exhibits unprecedented temperature-responsive optical properties for applications in thermochromic materials, thermal/photoresponsive switches, sun protecting glazing, photopatterning and temperature sensing labels.

1. Introduction

Liquid crystalline polymers (LCPs) comprising azobenzene and/or cholesterol moieties with optical tunability in the visible or the near-infrared region are of interest for controlling and processing light of active components in display, sensory and telecommunication devices.[1-3] Azobenzene LCPs are well known as stable photoresponsive liquid crystal (LC) materials, and their photochemical phase transition[4, 5] between the liquid crystalline phase and the random state and birefringence are very useful parameters for optical photonic crystal switching[1, 6-8] retarders[9], compensators[10], spectrum band filters[11] and efficient polarizers[12].[13] Cholesteric LCPs possess chiral mesophases with tunable helical pitch that provides intriguing optical and electro-optic properties[14], selective light reflection[15] and ferroelectricity, and have broad applications in electronic-controlled elastomers[16], light reflection materials and chiral recognition.[17]

There are a few examples of acrylate and methacrylate copolymers containing both azobenzene and cholesterol synthesized and evaluated for third-order non-linear optical properties. Different substituents attached to the azobenzene moieties such as nitro groups influence third-order non-linear susceptibility.[18] However, when azobenzene and chiral molecules capable of forming cholesteric mesophases are incorporated in the same system, different levels of selectivity to irradiated light (UV or otherwise) has been demonstrated.[19] While most of these cholesterol and azobenzene copolymers exhibit ϕ- ϕ*, π-π* and n-π* electronic transitions, the optical reflections present limited range of wavelengths and thermo-responsive optical properties have not been explored.[19, 20] Thus modular, simple and general synthetic methods towards well-defined copolymer architectures comprising both functional azobenzene and cholesterol moieties with good control over composition, monomer distribution and molecular weights are currently lacking. These copolymers will present unique self-assembled mesophase behavior and here-to-fore unknown temperature-responsive optical properties and serve as a versatile platform for soft photonic crystals, lithographic materials, surface modifiers and optoelectronics.[3], [21]

Recently, we carried out extensive studies on side chains liquid crystalline brush-like copolymers. For instance, liquid crystalline brush like block copolymers (LCBBCs) comprising side chain cholesteryl molecules and polyethylene glycol (PEG) side chain molecules display co-existence of smectic A (SmA) mesophase (3-7 nm) while PEG side-chains microphase segregate

into a lamellar or cylindrical domains (40- 75 nm).[22] However, in the case of a random copolymer of the same monomers (cholesterol and PEG), cholesteryl side chain formed smectic mesophase (3-7 nm LC layers) PEG side chains microphase segregated into domains lacking long-range order (10- 15 nm).[23] Furthermore, with increasing temperature, smectic LC mesophases transition into 1D photonic cholesteric (N*) mesophase reflecting light in the visible region (450 - 470 nm), while co-existing with microphase segregated of PEG domains. Furthermore, we explored liquid crystalline-liquid crystalline (LC-LC) competing interactions and the microphase segregation within brush-like random terpolymers comprising cholesterol, cyanobiphenyl and PEG monomers. In these systems, PEG behaved as an internal plasticizer as well as a physical junction-point and afforded the system some elastomeric features. We observe that the introduction of a cyanobiphenyl mesogenic species in the terpolymer results in altering of the pitch length of N* mesophase and hence change in light reflecting optical properties.[24] However, the photonic reflections of the terpolymer system was limited to the visible range of 400-550 nm .

Herein, we report (1) modular synthesis of new homopolymers containing functional azobenzenes, (2) copolymers comprising functional azobenzenes and cholesterol and (3) terpolymers comprising functional azobenzene, cholesterol and PEG side chains. The addition of azobenzene comonomers and PEG induces unique levels of cooperative interactions, including cholesterol-azobenzene (LC-LC) interactions and plasticization of PEG, which in turn acts like a tuning knob for the pitch length of thermally responsive cholesteric helices resulting in wide range of wavelength coverages from the visible range to near infrared. Furthermore, the effect of the presence of a chiral co-liquid crystalline monomer (azobenzene) with functional groups of varying polarity within copolymers and terpolymers and effect of temperature on spectral range of copolymers and terpolymers will be considered.[25, 26] Due to the combined effects of LC-LC interactions, PEG plasticization, polarity and functionality of azobenzene derivatives and responsive features of cholesteric helixes, this new copolymer and terpolymer platform presents temperature responsive and reversible1D photonic materials with spectral range of visible to near infra-red reflections, which is not feasible from either azobenzene homopolymers or cholesteric homopolymers.

2. RESULTS AND DISCUSSION

2.1 Synthesis and Characterization

Monomers: The monomers NBCh9[27] and NBMPEG[23] are synthesized according to previously reported procedures. New side chain azobenzene monomers with different terminal functional groups, hydrogen (-H), cyano (-CN), nitro (-NO_2) and methoxy (-OCH_3) are synthesized in three steps using modified literature procedures and details are as described in the supporting information (Schemes S1-S3). The purity, structure and composition of all the monomers are confirmed by ^{1}HNMR and other characterization methods (Figure S1) and these monomers are labelled $NBAz_{12}$-X (X=H, CN, NO_2, OCH_3).

Homopolymers and Copolymers: Using modified Grubbs second generation catalyst, a series of copolymers of NBCh9 and $NBAz_{12}$-X (X=H, CN, NO_2 or OCH_3) are synthesized (Figure 1) by ROMP using CH_2Cl_2 as a solvent. The polymerization reaches completion within 25-30 minutes taking into account the two monomers (NBCh9 and $NBAz_{12}$-X) exhibit different rates of polymerization (Figure S4). We expect gradient distribution of NBCh9 and $NBAz_{12}$-X (X=H, CN, NO_2 or OCH_3) as compared to nearly random distribution of NBCh9 and NBMPEG monomers with similar rates of polymerization.[23] The terminology CP-85 will be used, where CP represents the copolymer and 85 represents the wt % of cholesteric monomer (NBCh9).

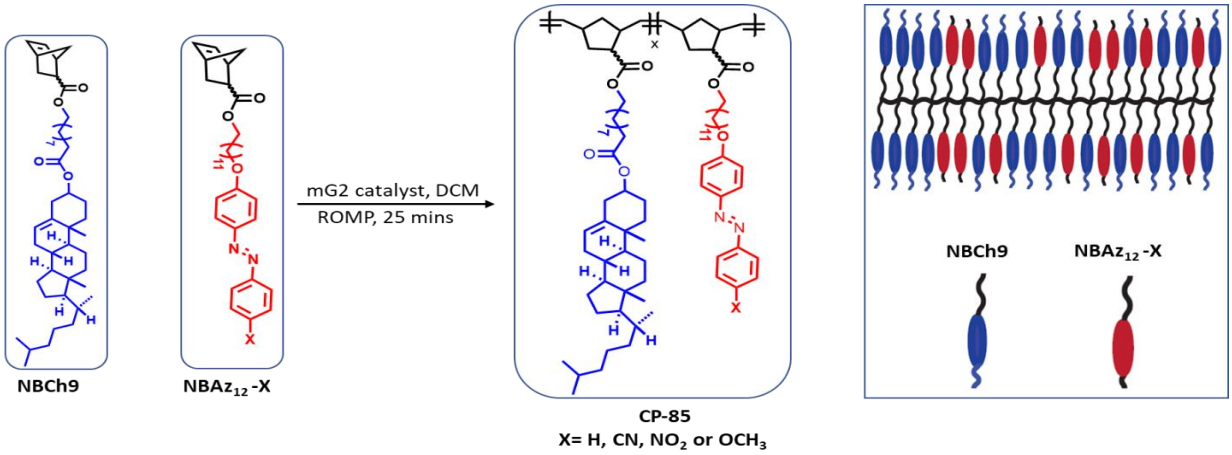

Figure 1: Synthesis of Copolymer (CP-85) by ROMP using side-chain functionalized NBCh9 and NBAz12-X (X=H, CN, NO_2 or OCH_3) monomer and illustration of CP-85 architecture.

A representative ^{1}H NMR spectrum of CP-85 (X=CN or OCH_3) is shown in Figure S2, the peaks 7.0 and 4.5 ppm labelled a and b (CP-85 structure in Figure 1 and Figure S2) correspond to two protons for NBAz12-X and one proton for NBCh9 respectively. The weight percentage of each monomer in the copolymer is determined by comparing the integration of these two peaks. Table 1 summarizes the molecular characterization of the homopolymers and copolymers. Ring opening metathesis polymerization of these monomers yields polymers with comparable molecular weights

with narrow polydispersity. We synthesized other compositions of copolymers of 50 wt% NBCh9 and 50 wt% NBAz12, (X= H, CN, OCH_3 and NO_2) (CP-50).

Terpolymers: Recently, we explored comb-shaped terpolymers from ROMP of NBCh9, NBMPEG and cyano biphenyl functionalized norbornene (NBCB12).[24] Within the terpolymers, inclusion of cyano biphenyl monomer resulted in elongation of cholesteric helices arising from Ch9 derivatives, which led to bathochromic (red) shift due to cholesterol-cyanobiphenyl interactions. Here we demonstrated the significance of PEG side chains as an internal plasticizer while improving the processability of the terpolymer films and tuning of helical pitch leading to hypsochromic (blue) shift. While these polymers exhibit good mechanical integrity, they are limited to the wavelength range between 400- 550 nm.[24] To overcome this shortcoming we synthesized a series of novel terpolymers (Figure 2 and Table 1) having NBCh9, NBMPEG and new azobenzene monomers ($NBAz_{12}$-X (X=H, CN, NO_2, OCH_3).

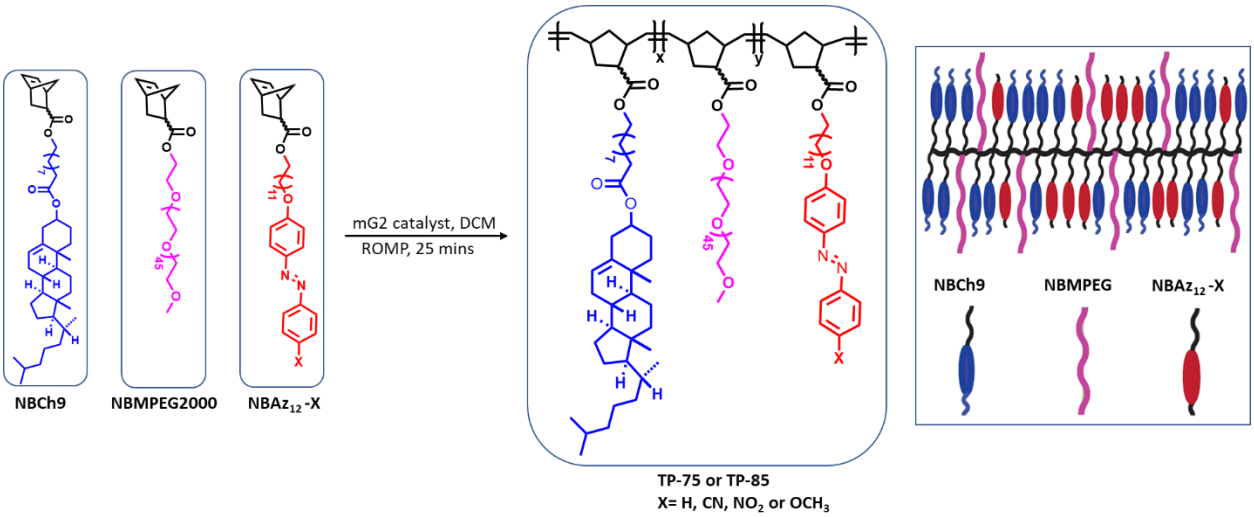

Figure 2: Synthesis of Terpolymer (TP-75 or TP-85) by ROMP using side-chain functionalized NBCh9, NBMPEG and $NBAz_{12}$-X (X=H, CN, NO_2 or OCH_3) monomer and illustration of TP-75 architecture.

Table1: Polymer Composition and Molecular Weight Characterization

Entry[1]	Polymer Description	Weight Percentage [2] (From ^{1}HNMR)			Theo. Mw kDa/mol	M_n [3] kDa/mol; $Đ_M$(PDI)
		$NBCh_9$	$NBAz_{12}$	NBPEG		
TP-75, X= H	P($NBCh_9$-r-$NBAz_{12}$-X-r-NBPEG), X= H	76.82	9.14	14.04	60.1	71.0 (1.05)
TP-85, X= H	P($NBCh_9$-r-$NBAz_{12}$-X-r-NBPEG), X= H	83.75	9.80	6.45	61.0	72.3 (1.07)
CP-85, X= H	P($NBCh_9$-r-$NBAz_{12}$-X), X= H	85.52	14.48	- -	60.3	76.2 (1.07)
$PNBAz_{12}$, X = H	P($NBAz_{12}$-X), X= H	- -	100	- -	60.3	73.7(1.05)
TP-75, X= CN	P($NBCh_9$-r-$NBAz_{12}$-X-r-NBPEG), X= CN	76.96	9.71	13.33	60.9	68.3 (1.08)
TP-85, X= CN	P($NBCh_9$-r-$NBAz_{12}$-X-r-NBPEG), X= CN	84.81	9.48	5.71	61.3	70.9 (1.07)
CP-85, X= CN	P($NBCh_9$-r-$NBAz_{12}$-X), X= CN	86.31	13.86	--	60.9	55.8 (1.17)
PNBAz12, X = CN	P($NBAz_{12}$-X), X= CN	--	100	--	60.2	74.9 (1.22)
TP-75, X= NO_2	P($NBCh_9$-r-$NBAz_{12}$-X-r-NBPEG), X= NO_2	76.33	10.45	13.22	60.8	63.3 (1.09)
TP-85, X= NO_2	P($NBCh_9$-r-$NBAz_{12}$-X-r-NBPEG), X= NO_2	83.37	10.21	6.42	61.0	65.4 (1.13)
CP-85, X= NO_2	P($NBCh_9$-r-$NBAz_{12}$-X), X= NO_2	84.22	15.78	--	61.3	93.6 (1.07)
PNBAz12, X = NO_2	P($NBAz_{12}$-X), X= NO_2	--	100	--	60.8	72.4 (1.06)
TP-75, X= O CH_3	P($NBCh_9$-r-$NBAz_{12}$-X-r-NBPEG), X= OCH_3	77.18	9.45	13.37	60.6	70.9 (1.08
TP-85, X= OCH_3	P($NBCh_9$-r-$NBAz_{12}$-X-r-NBPEG),	84.38	10.75	4.87	60.1	71.2 (1.06)
CP-85, X= OCH_3	P($NBCh_9$-r-$NBAz_{12}$-X), X= OCH_3	84.39	15.61	--	61.0	54.1 (1.16)
PNBAz12, X= OCH_3	P($NBAz_{12}$-X), X= OCH_3	--	100	--	60.7	66.8 (1.15)
LCRBC_85*	P($NBCh_9$-r-NBPEG)	84.47	--	15.53	60.3	56.8 (1.04)
PNBCh9**	PNBCh9	100	--	--	61.0	60.3 (1.03)

[1]**Terpolymers are labeled as TP-75 (X=H, CN, NO_2 or OCH_3) where 75 stands for weight fraction of cholesteric monomer and X refers to the type of azobenzene monomer in the**

terpolymer. Copolymers are labeled as CP-85 (X=H, CN, NO_2 or OCH_3) where 85 stands for weight fraction of cholesteric monomer and X refers to the type of azobenzene monomer in the copolymer.

[2] Weight percentage of each monomer in random terpolymer and copolymer samples are determined by ^{1}HNMR integrations of the peaks at 4.6, 3.36 and 6.99 or 7.89 ppm corresponding to NBCh9, NBMPEG and NBXAz$_{12}$ monomers, respectively.

[3] Determined by GPC with ELSD detector, where THF was used as eluent and polystyrene (PS) standards were used to construct a conventional calibration.

The terpolymers are labelled TP-75, (X=H, CN, NO_2, and OCH_3) and TP-85, (X=H, CN, NO_2, and OCH_3) where 75 and 85 represents the wt% of NBCh9 monomer (Table1), respectively. The synthesis of narrow molecular weight terpolymers is feasible because Grubbs catalyst has a steric/functional group tolerance, stable and capable of polymerizing monomers with dissimilar moieties of different side chain lengths into copolymers with hierarchical architectures.[24, 28-30] Composition of 75 and 85 wt% of NBCh9 is of significance which is to enhance terpolymer to self-assemble into cholesteric mesophase N*. The monomer NBMPEG is varied between 5 and 15 wt% to provide the mechanical integrity and easy processability of the polymer films. Inclusion of NBAz$_{12}$-X (X=H, CN, NO_2 and OCH_3) results in a scaffold within which LC-LC interactions of NBCh9 and the azobenzene monomers (NBAz$_{12}$-X) enables variations of photonic properties. The compositions in TP-75 and TP-85 are determined by integrating characteristic peaks of NBCh9 (one proton at 4.6 ppm, labelled a), NBMPEG (three protons at 3.36 ppm labelled b) and NBAz$_{12}$-X (X=H, CN, NO_2 or OCH_3) (two protons at 7.0 ppm, labelled c) in ^{1}H NMR spectra and by comparing the ratio of their integration values (Figure S3).

2.2 Thermal Properties

Thermal transitions in homopolymers, copolymers and terpolymers were investigated using differential scanning calorimetry (DSC) and shown in Figures 3-4 and Figures S5-S10. Samples were first heated to 150 °C at a rate of 10 °C/min to remove the thermal history. Data from the subsequent first cooling cycle for azobenzene homopolymers PNBAz$_{12}$-X (X= H, CN, NO_2 or OCH_3) are shown in Figure S6. The azobenzene homopolymers had two transitions: polynorbornene glass transition (20–54 °C) and LC clearing transition (53-101 °C). PNBAz$_{12}$-H

had the lowest LC clearing transitions (53.24° C) while the highest value was observed in $PNBAz_{12}$-OCH_3 (100.91°C). These homopolymers had the same norbornene backbone and similar molecular weight and hence the thermal transitions T_g and T_{LC} were mainly dependent on the side/terminal groups.[31] While LC transition temperature was noticeably higher for azobenzene homopolymers bearing -OCH_3, -CN or -NO_2 functional groups compared to $PNBAz_{12}$-H, there was no clear trend in the thermal transitions.[32]

Copolymer containing NBCh9 and NBAz12-X (X=H, OCH_3, CN, NO_2) showed three thermal transitions: polynorbornene backbone glass transition (T_g) and two distinct LC transitions (T_{LC1} and T_{LC2}), similar to those witnessed in PNBCh9 (Figure S5 and Figure S7).[33] In comparison, copolymer containing NBCh9 and NBMPEG (LCRBC_85) which showed three transitions: polynorbornene backbone glass transition (T_g) and two distinct LC transitions (T_{LC1} and T_{LC2}) with depressed crystallization temperature attributed to PEG side chains (Figure S8).[23] The thermal properties of CP-50, X= CN and OCH_3 (Figure S8) were similar to those of azobenzene homopolymers and had two transitions: glass transition T_g and LC clearing transition (T_{LC}) .

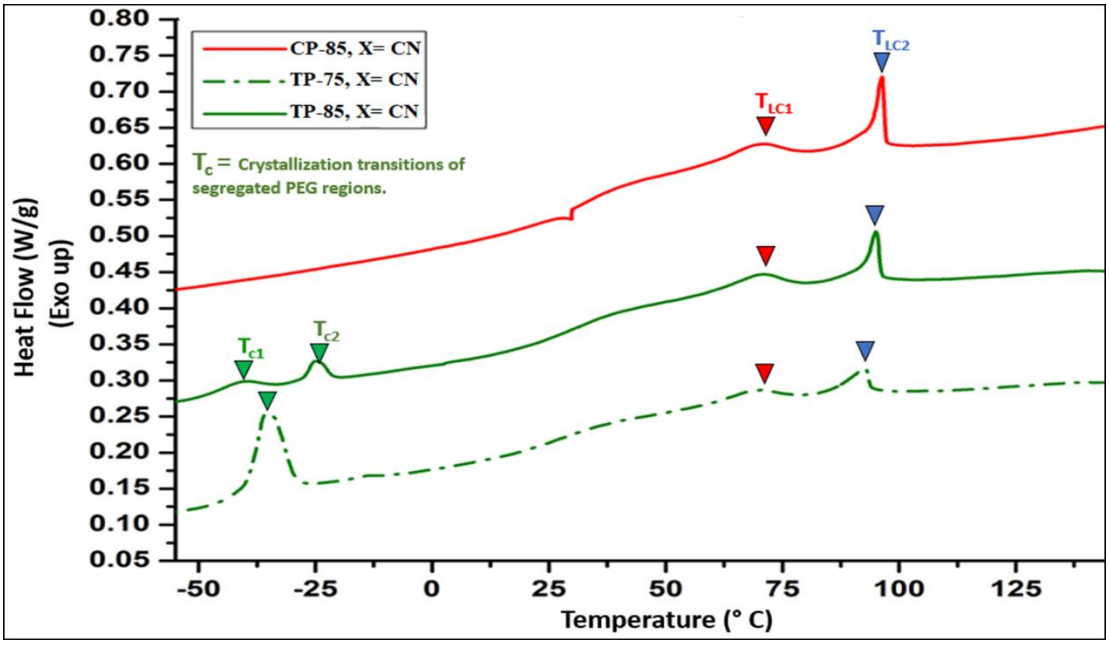

Figure 3: **The first cooling cycle DSC thermogram of TP-85 (X=CN), TP-75 (X=CN) and CP-85 (X=CN) with a cooling rate of 10 °C/min. Four different transitions were observed: (i) PEG crystallization transition (T_c) was present in TP systems but was absent in CP systems;**

(ii) glass transition temperature (T_g) of polynorbornene backbone and LC mesophase transition temperatures; (iii) T_{LC1} and (iv) T_{LC2}.

The terpolymers (TP-85-X and TP-75-X, X=H, CN, NO_2 or OCH_3) underwent three transitions during the first cooling cycle as shown by DSC scans in Figure 3, 4 and S10 , which were similar to those observed in copolymers of NBCh9 and NBMPEG (LCRBC-85, Figure S9): T_g transition, PEG crystallization transition (T_c), and two distinct LC transitions (T_{LC1} and T_{LC2}).[23] Depressed PEG crystallization (T_{C1} and T_{C2}) observed at -20 to -45 °C in both terpolymers (Figures 3 and 4 and S10) was due to nanoconfined hierarchical structures.[22, 24, 34,35]

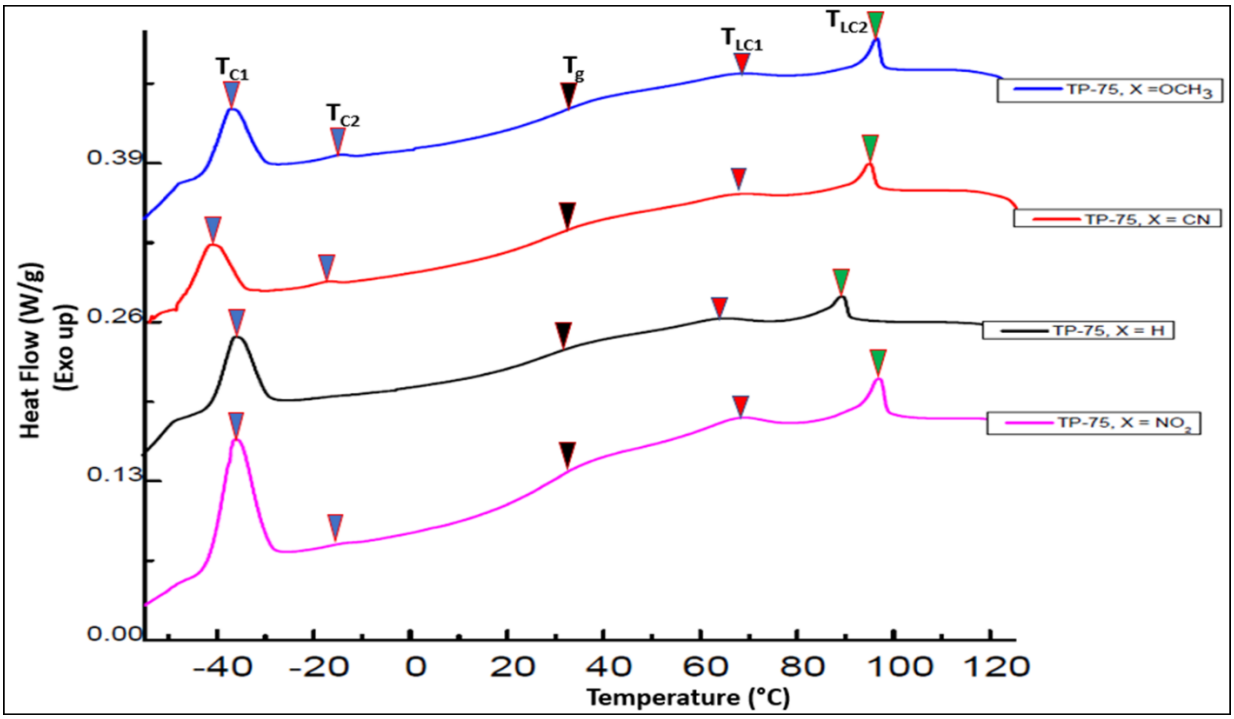

Figure 4: The first cooling cycle DSC thermogram of TP-75 (X=NO_2, H, CN and OCH_3), with a cooling rate of 10 °C/min.

2. Microstructure Analysis of Cholesteric-Azobenzene Polymers.

Small-angle X-ray scattering (SAXs) diffractograms obtained at room temperature for $PNBAz_{12}$, X=H, CN, NO_2 and OCH_3 homopolymers present two types of reflections arising from

smectic LC order (q_{LC1}, q_{LC2}), Figure S11. Table S1 summarizes the d-spacings of smectic layers in PNBAz$_{12}$, X=H, CN, NO_2 and OCH_3 recorded at room temperature. The side-chain lengths for the NBAz$_{12}$, X=H, CN, NO_2 and OCH_3 are calculated by 3D ChemDraw software to compare with experimentally obtained layer spacings. For PNBAz$_{12}$, X=H, CN, NO_2, OCH_3 the ratio of d_1 and d_2 is 1: ½ which clearly shows that d_2 is second order of d_1. The calculated side-chain lengths for PNBAz12, X=CN and NO_2 is a half that of d_1 and approximately equal to that of d_2 suggesting interdigitated bilayer and monolayer smectic arrangements respectively, while for PNBAz$_{12}$, X=H and OCH_3, the calculated side-chain lengths have no correlations with the d-spacings obtained experimentally which indicates the existence of more than a single type of smectic layer arrangements. The results obtained is in agreement to what is documented in literature for side chain liquid crystalline polymers (SLCPs), where interdigitated smectic layers can occur when mesogens bear a strong polar terminal group such as cyano (- CN) or nitro (-NO_2) due to dipole interactions of mesogens between the polymer chains or due to strong asymmetry in the shape of mesogens.[36, 37]

a) **b)**

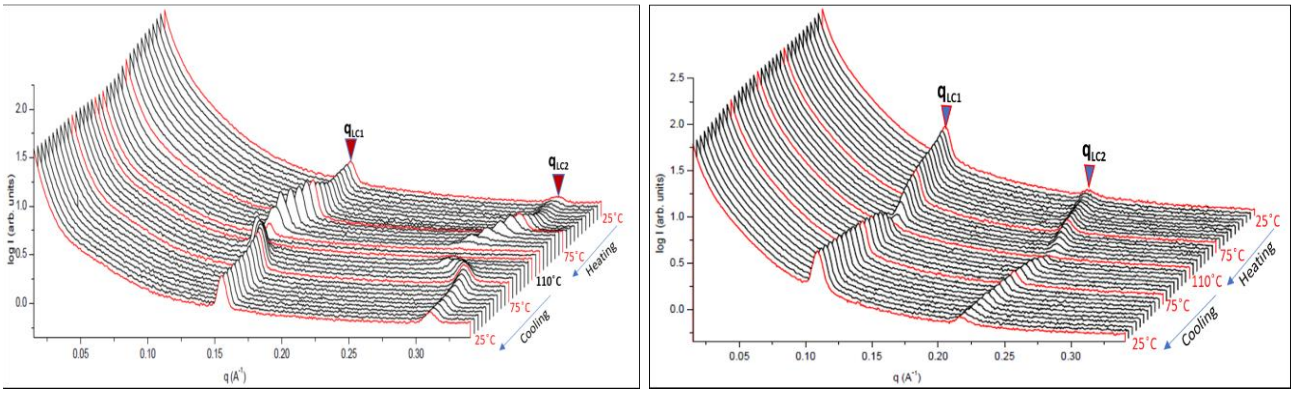

Figure 5. (a) Temperature dependent 1D SAXS of PNBAz12, X=OCH_3 and (b) PNBAz12, X=CN. The samples are compression molded at different temperatures with reference to T_{LC} and quenched to room temperature.

Temperature dependent SAXS measurements for PNBAz12, X=H, OCH_3, CN and NO_2 are presented in Figure 5 and Figure S13. With increase in temperature, the intensity of reflection peaks corresponding to d_1 and d_2 increases and start decreasing on approaching the T_{LC}, finally clears slightly above T_{LC}. Reflections q_{LC1} and q_{LC2} re-appear on cooling back from isotropic to

smectic transition (T_{LC}) for all the homopolymers, this is in agreement with thermal transitions (T_{LC}) observed in DSC (Figure S6). For example, the intensities of peaks q_{LC1} and q_{LC2} for $PNBAz_{12}$, X=OCH_3 (Figure 5) increases with temperature up to 95 °C then gradually weakens and finally clears into the isotropic state around 105 °C.

In copolymers, CP-85, X=H, CN NO_2 and OCH_3, at room temperature three reflections corresponding to q_{LC1}, q_{LC2} and q_{LC3} are observed (Figure S12). Layer spacings d_1, d_2 and d_3 (Table S2) for CP-85, X=H, CN, NO_2 and OCH_3 indicates that these reflections non-correlated which implies coexistence of smectic mesophases. In previous studies, we showed that the cholesteryl side chain length is 3.34 nm which compares to d_2 reflection in all CP-85 copolymers (Table S2), suggesting existence of monolayer smectic mesophase (S_mA).[33] The domain spacings of d_1 and d_3 in these copolymers suggest existence of bilayer and interdigitated smectic mesophase, respectively, this largely depends on the spacer length (12 methylene) in the azobenzene mesogen (Az_{12}). The existence of different smectic mesophase has been attributed to LC mesogens, length of spacer moiety and backbone decoupling in thermotropic LC polymers.[23, 38]

a) b)

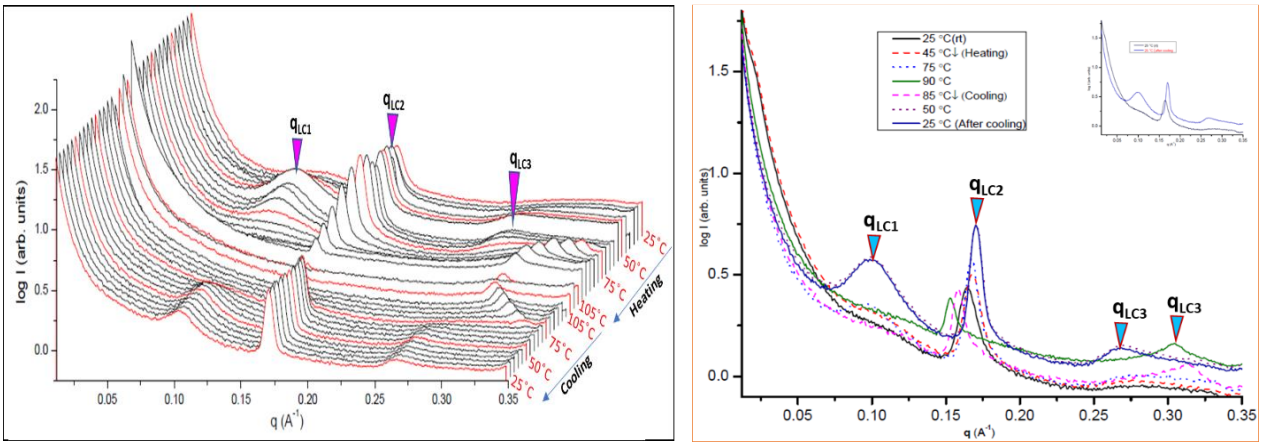

Figure 6. a) Temperature dependent 1D SAXS of CP-85 (X= OCH_3) compression molded at 104 °C and quenched to room temperature and b) SAXS profiles measured in situ depicting thermal annealing of CP-85 (X= CN).

In Figure 6 which represents Temperature dependent 1D SAXS of CP-85, X=OCH_3, shows that intensities of the reflection q_{LC1}, q_{LC2} and q_{LC3} increase upon heating. The reflection q_{LC1} clears above 75 °C and q_{LC2} clears above 105 °C, while q_{LC3} change reflections shift to higher q values

and intensity decreases at 105 °C but does not disappear completely. For CP-85, X=OCH_3 (Figure 6), LC transition from smectic to cholesteric mesophase then to isotropic above 105°C is expected and is in general agreement with DSC data (Figure S7). Temperature SAXS depicts the thermal annealing of CP-85, X=CN (Figure 6b), the intensities of reflections especially q_{LC1} increased significantly and stabilized even after cooling to room temperature. The increase in the intensities is attributed to increase in LC ordering in the copolymers. At higher temperatures q_{LC3} shifts slightly to a higher value signifying the LC mesogens becomes more labile and different levels of molecular packing in these copolymers. In these copolymers, some residual smectic phase may co-exist with the cholesteric phase as noted previously with other copolymers. Since it is challenging to characterize cholesteric mesophase using SAXS due to limited q-range, UV-Vis reflectance may be used to show light reflections from cholesteric domains as discussed in the next section.[23, 24, 39]

a)

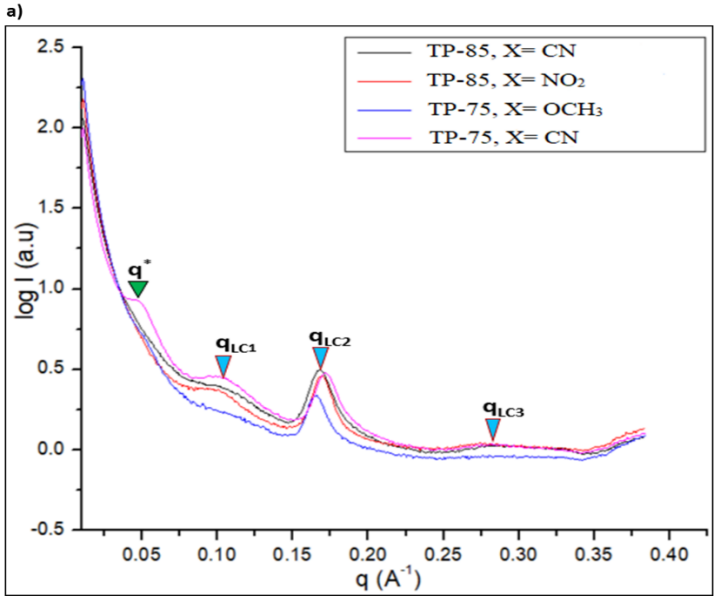

b)

Polymer	d_1 (nm)	d_2 (nm)	d_3 (nm)	d_4 (nm)
TP-85, X= CN	-	6.09	3.72	2.20
TP-85, X= NO_2	-	6.32	3.71	2.28
TP-75, X= OCH3	12.25	5.98	3.84	2.18
TP-75, X= CN	12.73	6.14	3.64	2.20

Figure 7. a) Room temperature 1D SAXS for terpolymers TP-85, X=CN or NO_2 and TP-75, X=CN or OCH_3 and **b) Table comprising domain (d) spacings for terpolymers.**

Room temperature small angle X-Ray (SAXS) diffractograms of TP-85, X=CN or NO_2 and TP-75, X=CN or OCH_3 and domain spacings (d-spacings) are as observed in Figure 7. The observed data shows different levels of intermolecular packing and LC ordering. The broad q* correspond to PEG domains at ~12.73nm and is consistent with previous studies while the three LC reflections with domain spacings at d_{LC1} = 6.14nm, d_{LC2} = 3.67nm and d_{LC3} = 2.2 nm

corresponding to phases emanating from Ch9 and Az_{12}-X units respectively.[24] The d-spacing results suggests smectic polymorphism: monolayer and bilayer within the same system. From literature, it has been shown that polar electron withdrawing (-NO_2 or -CN) groups induces a more ordered antiparallel or interdigitated packing due to strong dipole-dipole interactions between the terminal groups.[36, 37, 40]

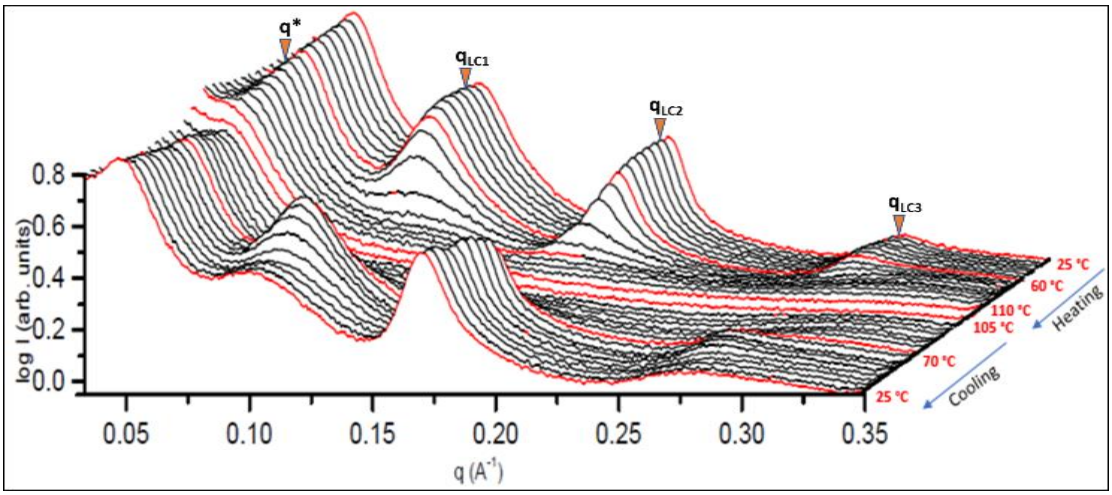

Figure 8. Temperature dependent 1D SAXS of TP-75 (X=CN) compression molded at 90 °C and quenched to room temperature.

Temperature dependent SAXS investigation of TP-75, X=CN shows four reflections due to PEG domains and LC transitions. The LC reflections, indicative of co-existing smectic phases maintain their intensities till about 95°C and gradually clear above 105 °C while the microphase segregated PEG domains remain intact, Figure 8. The disappearance of reflections at q_{LC1}, q_{LC2} and q_{LC3} progressively disappears which is coincident to cholesteric-isotropic mesophase transition observed in DSC. A similar trend is observed in all other terpolymers (Figure S14). Thus, temperature dependent SAXS for the terpolymers indicates a clear transition from smectic to cholesteric mesophase then to isotropic, due composition, molecular distribution and multicomponent nature in this system.[24, 38]

3. Photonic properties

Cholesteric liquid crystalline polymers are characterized with continuous twisted arrangements of chiral mesogens (helical cholesteric mesophase, N*) featuring 1D photonic

properties that can be tuned by use of a stimulus such as heat, light or temperature. In our previous publications, we showed that cholesteric polymers can be tuned to reflect different wavelengths (colors) by use of temperature.[23, 24, 33]

For UV-Vis reflection measurements, solid polymer powders are compression molded and annealed between two Kapton films at different temperatures with reference to T_{LC1} or T_{LC2}, quenched to room temperature to kinetically trap the cholesteric mesophase using cold air or liquid nitrogen to a temperature below T_g that preserves the cholesteric mesophase while retaining the reflected color.[39] UV-Vis spectra in the reflectance mode for PNBCh9 (a control)[33] annealed at 105 °C ($T< T_{LC2}$) and 88 °C ($T< T_{LC1}$) (Figure S5) and subsequently quenched to room temperature with a stream of cold air displays two maxima at 415 and 527 nm (Figure S15) respectively. This shows that cholesteric homopolymer is thermal responsive and tuning its helical pitch leads to observed optical properties.

Four different azo benzene derivatives have been prepared with functional groups in the para position of the phenyl group including -H, $-OCH_3$, -CN and $-NO_2$, which is in order of increasing electron withdrawing capabilities. Unlike other acrylate based azo system, the homopolymers show two peak maxima (390 - 617 nm) (Figure S16) that can be attributed to π- π^* and n- π^* electronic transitions respectively. Also, unlike polyacrylate containing azo benzene, cyano and nitro groups that are more electron withdrawing show increasing red shift. When $PNBAz_{12}$, $X=OCH_3$ (Figure S17) is annealed at temperature near its the liquid transition temperature (T_{LC}) there was no significant shift in the wavelength maxima, this indicates that the azobenzene homopolymers are not thermal responsive due to the smectic mesophases that exist in the homopolymer.

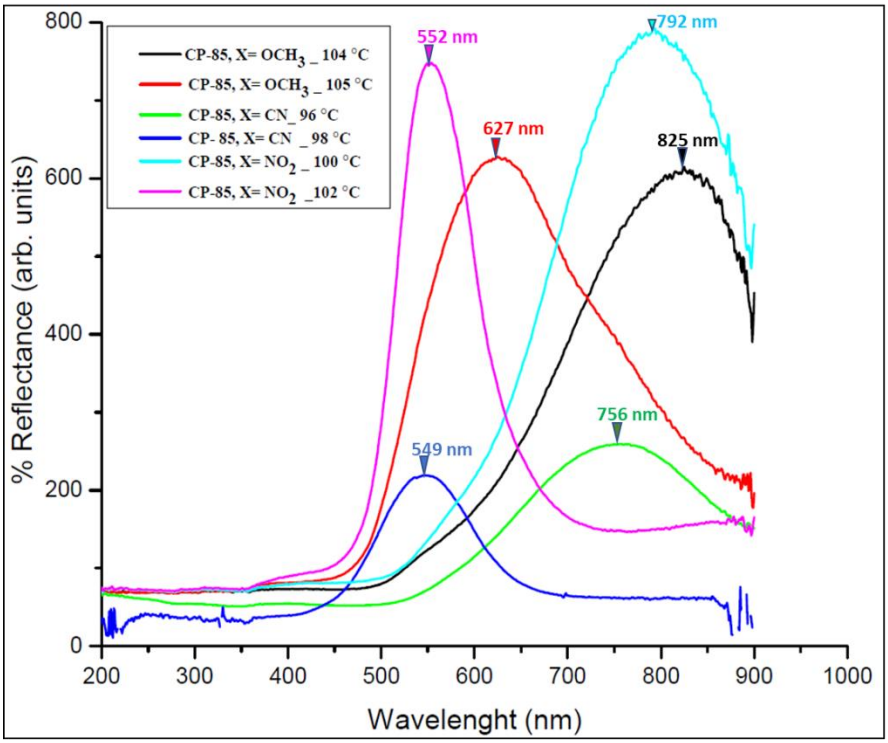

Terpolymer	λmax (nm)
CP-85, X= NO_2 (102 °C)	552
CP-85, X= NO_2 (100 °C)	792
CP-85, X= CN (98 °C)	549
CP-85, X= CN (96 °C)	756
CP-85, X= OCH_3 (105 °C)	627
CP-85, X= OCH_3 (104 °C)	825

Figure 9: Light reflection of CP-85 (X=NO_2, CN and OCH_3) film samples prepared by compression molding at different temperatures (table alongside).

The LC- LC interactions between the LC mesogens (Ch9 and Az12, X=H, CN, NO_2 or OCH_3) when present in the same domain or across the interface of the copolymer leads to a wider range of colors reflected.[41, 42] The UV-Vis spectra of the cholesteric-azobenzene copolymers (CP-85, X=H, CN, NO_2 or OCH_3) comprising of 85 wt% NBCh9 and 15 wt% $NBAz_{12}$, X=H, CN, NO_2 and OCH_3 are shown in Figure 9 and Figure S18. The pitch of the cholesteric mesophase is influenced by temperature which renders these copolymers thermochromic with a wider cover of optical range from the visible to near infrared range compared to smectic mesophases within Azo homopolymers.

Increase in temperature causes blue shift in CP-85, X=H, CN, NO_2 or OCH_3 while decrease in temperature leads to a red shift. [15, 43] For example, CP-85, X=OCH_3 (Figure 9) shows a reflection band around the near-IR region of λ_{max} ~ 825 nm when the sample is heated and annealed at 104 °C and on annealing the sample at 105 °C the film changes from deep red to greenish color with λ_{max}, ~ 612 nm. The shift of reflection bands from near-IR to visible region is reversible that if the samples are heated to slightly above T_{LC2}, cooled slowly and then annealed at optimal temperatures

(Figure 9). From the UV-Vis spectra of copolymers (Figure 9), a change of one terminal group to other results to a completely shift of the reflected bands, this could be attributed to the difference in elastic constants of these groups (-H, -CN, -NO_2 and -OCH_3).[44]

The results obtained shows clearly the effect temperature has on the helical twisting power (HTP) of these samples. When this effect of heat combines with one induced from the polarity of the terminal groups, different levels of molecular or LC- LC interactions are expected hence, the unique optical properties from these copolymers. Highly polar groups such as NO_2 have a strong influence on the molecular interactions and order parameter of the LC mesogens in the copolymer leading to variation in the cholesteric helical pitch length.[3, 45] The optical properties of CP-50, X= OCH_3 and NO_2 (Figure S19) were similar to those obtained from azobenzene homopolymers.

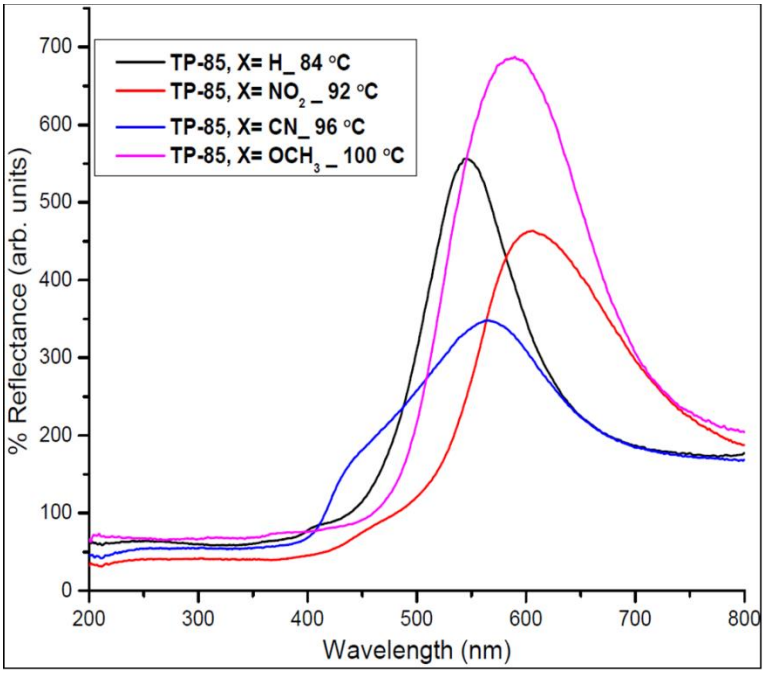

Terpolymer	λmax (nm)
TP-85, X= H (84 °C)	548.5
TP-85, X= NO_2 (92 °C)	608.8
TP-85, X= CN (96 °C)	568.0
TP-85, X= OCH_3 (100 °C)	590.4

Figure 10: Light reflection of TP-85 (X=H, NO_2, CN and OCH_3) film samples prepared by compression molding at distinctive temperatures depending on the liquid crystalline transition temperature (T_{LC2}).

In our recent studies, we explored the effect of LC-LC interactions on the helical structure of the cholesteric mesophase by introducing cyanobiphenyl monomer in the comb terpolymers, the LC monomer induced elongation of cholesteric helices leading to a red shift.[24]. These terpolymers were limited to the optical range they could cover in the electromagnetic spectrum,

i.e., 400- 550 nm, this led to synthesis of the present new cholesteric- azobenzene liquid crystalline terpolymers that could cover a wider range from the visible to near infrared.

The interaction between the azobenzene and cholesteric units tunes the pitch length of cholesteric helices leading to a wider range of optical wavelengths observed from the UV-Vis spectrum of the cholesteric-azobenzene terpolymers, Figures 10. By comparing TP-85 terpolymer having 85 wt% of NBCh9, 10 wt% of NBAz12, X=H, CN, NO_2 or OCH_3 and 5 wt% of PEG (Figure 10) and TP-75 which contains 75 wt% of NBCh9, 10 wt % of NBAz12, X=H, CN, NO_2 or OCH_3 and 15 wt% of NBMPEG (Figure S20), the effect of PEG is evident in that PEG causes blue shift upon inclusion in the terpolymers. Thus, PEG acts as a plasticizer altering the helical pitch of the cholesteric mesophase to shift the λ_{max} to a lower wavelength.

Unlike norbornene based homo(azo)polymers, terpolymers do not show any trends in the reflection spectra that can be correlated with electron withdrawing or donating nature of the substituents on the azo group. This may be due to the azo groups being incorporated into the cholesteric helix and the optical reflections are due to cholesterol-azobenzene interactions rather than just the azobenzene reflections. For instance, in TP-75 or TP-85 which contains $NBAz_{12}$-NO_2 monomer with dominant electron withdrawing nitro group, a red shift is observed with λ_{max} of ~ 587 nm for TP-75, X=NO_2, (Figure S20) and ~ 610 nm for TP-85, X=NO_2, (Figure 10). Substituting this monomer with one containing more electron donating species such as $NBAz_{12}$-H the reflectance band shifts towards the blue region, ~ 550 nm for TP-85 or TP-75, X=H, (Figures 10 and S20). Copolymers of NBCh9 and NBMPEG (LCRBC-85, Table 1)[23] synthesized as a control could only record a blue shift of λ_{max}, ~415 nm (Figure S15).

The optical textures of the copolymers and terpolymers are further investigated using Polarized Optical Microscope (POM), where for CP-85, X= OCH_3 (Figure S21), green color reflection from sample is observed in POM after annealing sample at 85 °C for 24 h. The higher magnification POM images of CP-85, X= OCH_3 and TP-75, X= CN (Figure S21-22) shows cholesteric oily streaks and smectic mesophase.

The optical properties observed demonstrates that by manipulating monomer composition or stimuli such as temperature the helical pitch of the cholesteric mesophase can be tailored inducing short or long wavelength reflections as needed. Thus, the developed cholesteric-azobenzene copolymers could be potentially exploited in temperature sensing labels, photopatterning, advanced optics, photonics and tunable cholesteric lasers.

Conclusion

In this manuscript, we have demonstrated a general method to synthesize azobenzene and cholesterol copolymers and azobenzene, cholesterol and PEG terpolymers. The wide range of wavelengths is a result of cooperativity originating from the varying cholesteric pitch length due to LC-LC interactions in copolymers and LC-LC interactions along with PEG presence in terpolymers. LC transition temperatures from azobenzene homopolymers are observed to depend on the side/terminal groups on the azobenzene unit. Copolymers from cholesterol and PEG show depressed crystallization temperature attributed to PEG nanoconfinement. A similar observation is made for the terpolymers of cholesterol, azobenzene and PEG where liquid crystalline ordering provides sufficient confinement leading to suppression of PEG crystallization.

Microstructural analysis by SAXS in homopolymers, copolymers and terpolymers reveals interesting features. Some of the homopolymers (PNBAz12, X=CN and NO_2), bearing strong polar terminal groups cyano (- CN) or nitro (-NO_2) due to dipole interactions show interdigitated bilayer and monolayer smectic arrangements, respectively, correlated by experimentally obtained values and theoretically predicted values (ChemDraw 3D). In copolymers, T-SAXS indicates transitions from smectic to cholesteric to isotropic, which differs based on presence of different terminal groups on the azo unit. For the terpolymers, temperature resolved SAXS indicates transition from smectic to cholesteric mesophase then to isotropic, due composition, molecular distribution and multicomponent nature in this modular system.

Unlike azo homopolymer and other known azo copolymers, in these copolymers and terpolymers, LC- LC interactions between the LC mesogens cholesterol and azobenzene leads to a wider range of colors reflected. An increase in temperature leads to a hypsochromic shift while a decrease in temperature leads to bathochromic shift. The shift in reflections from near-IR to visible regions is reversible. Change in monomer composition or stimuli controls cholesteric mesophase helical pitch. Many applications as envisioned in the introduction can be expected from these new class of materials including photonics and temperature sensing labels.

Conflicts of interest

There are no conflicts to declare.

Acknowledgements

This work is supported by the National Science Foundation under DMR-1507045. The central instrumentation facilities at the Institute of Materials Science and Chemistry Department at UConn are acknowledged. The authors thank Prof. Steven Suib and his research group for help with UV−visible measurements. The authors thank Dr. Lalit Mahajan, Prof. Chinedum Osuji, Dr. Manesh Gopinadhan and Dr. Youngwoo Choo for useful discussions.

References

1. F. Qiu, W. Zhang, D. Yang, M. Zhao, G. Cao and P. Li, *Appl. Polym. Sci*, 2010, **115**, 146-151.
2. K. Rameshbabu and P. Kannan, *Polym. Int*, 2006, **55**, 151-157.
3. P.-C. Yang, C.-Y. Li, H. Wu and J.-C. Chiang, *Journal of the Taiwan Institute of Chemical Engineers*, 2012, **43**, 480-490.
4. D.-Y. Kim, S. Shin, W.-J. Yoon, Y.-J. Choi, J.-K. Hwang, J.-S. Kim, C.-R. Lee, T.-L. Choi and K.-U. Jeong, *Adv. Funct. Mater.*, 2017, **27**, 1606294.
5. A. Emoto, E. Uchida and T. Fukuda, *Polymers*, 2012, **4**, 150.
6. S. Kim, T. Ogata and S. Kurihara, *Polymer Journal*, 2017, **49**, 407.
7. A. Skandani, J. A. Clement, S. Tristram-Nagle and M. R. Shankar, *Polymer*, 2017, **133**, 30-39.
8. H. Yu, *Progress in Polymer Science*, 2014, **39**, 781-815.
9. R. Giménez, M. Millaruelo, M. Piñol, J. L. Serrano, A. Viñuales, R. Rosenhauer, T. Fischer and J. Stumpe, *Polymer*, 2005, **46**, 9230-9242.
10. U. Oertel, H. Mart, H. Komber and F. Böhme, *Optical Materials*, 2009, **32**, 54-61.
11. P.-C. Yang, Y.-L. Lu and C.-Y. Li, *Journal of Molecular Structure*, 2012, **1015**, 129-137.
12. L. Fang, G. Han, J. Zhang, H. Zhang and H. Zhang, *European Polymer Journal*, 2015, **69**, 592-604.
13. A. Airinei, N. Fifere, M. Homocianu, C. Gaina, V. Gaina and B. C. Simionescu, *International journal of molecular sciences*, 2011, **12**, 6176-6193.
14. A. Ryabchun, I. Raguzin, J. Stumpe, V. Shibaev and A. Bobrovsky, *ACS Applied Materials & Interfaces*, 2016, **8**, 27227-27235.
15. D.-Y. Kim, S.-A. Lee, M. Park, Y.-J. Choi, W.-J. Yoon, J. S. Kim, Y.-T. Yu and K.-U. Jeong, 2016, **26**, 4242-4251.
16. S. Vyawahare, S. Sitaula, S. Martin, D. Adalian and A. Scherer, *Lab on a Chip*, 2008, **8**, 1530-1535.
17. A. Ryabchun and A. Bobrovsky, *Advanced Optical Materials*, 2018, **6**, 1800335.
18. A. Bobrovsky, N. Boiko, V. Shibaev and J. Stumpe, *Journal of Photochemistry and Photobiology A: Chemistry*, 2004, **163**, 347-358.
19. A. Bobrovsky and V. Shibaev, *Journal of Photochemistry and Photobiology A: Chemistry*, 2005, **172**, 140-145.
20. A. Y. Bobrovsky and V. P. Shibaev, *Advanced Functional Materials*, 2002, **12**, 367-372.
21. Y. C. Teo and Y. Xia, *Macromolecules*, 2015, **48**, 5656-5662.
22. P. Deshmukh, S.-k. Ahn, L. Geelhand de Merxem and R. M. Kasi, *Macromolecules*, 2013, **46**, 8245-8252.
23. P. Deshmukh, S.-k. Ahn, M. Gopinadhan, C. O. Osuji and R. M. Kasi, *Macromolecules*, 2013, **46**, 4558-4566.
24. L. H. Mahajan, D. Ndaya, P. Deshmukh, X. Peng, M. Gopinadhan, C. O. Osuji and R. M. Kasi, *Macromolecules*, 2017, **50**, 5929-5939.
25. F. Qiu, W. Zhang, D. Yang, M. Zhao, G. Cao and P. Li, *Journal of Applied Polymer Science*, 2010, **115**, 146-151.
26. P. Weis and S. Wu, *Macromol Rapid Commun*, 2018, **39**.

27. S.-K. Ahn, L. T. Nguyen Le and R. M. Kasi, *J. Polym. Sci. A Polym. Chem*, 2009, **47**, 2690-2701.
28. Y. Shao, Y.-G. Jia, C. Shi, J. Luo and X. X. Zhu, *Biomacromolecules*, 2014, **15**, 1837-1844.
29. F. Niedermair, M. Sandholzer, G. Kremser and C. Slugovc, *Organometallics*, 2009, **28**, 2888-2896.
30. B. R. Sveinbjornsson, R. A. Weitekamp, G. M. Miyake, Y. Xia, H. A. Atwater and R. H. Grubbs, *Proc Natl Acad Sci U S A*, 2012, **109**, 14332-14336.
31. Z. Guo, Q. Li, X. Liu, J. Hu and L. Yang, *Liquid Crystals*, 2016, **43**, 91-101.
32. K. Rameshbabu, P. Kannan, R. Velu and P. Ramamurthy, *Liquid Crystals*, 2005, **32**, 823-832.
33. S.-k. Ahn, M. Gopinadhan, P. Deshmukh, R. K. Lakhman, C. O. Osuji and R. M. Kasi, *Soft Matter*, 2012, **8**, 3185-3191.
34. P. Huang, L. Zhu, Y. Guo, Q. Ge, A. J. Jing, W. Y. Chen, R. P. Quirk, S. Z. D. Cheng, E. L. Thomas, B. Lotz, B. S. Hsiao, C. A. Avila-Orta and I. Sics, *Macromolecules*, 2004, **37**, 3689-3698.
35. Y. Zhou, S.-k. Ahn, R. K. Lakhman, M. Gopinadhan, C. O. Osuji and R. M. Kasi, *Macromolecules*, 2011, **44**, 3924-3934.
36. C. T. Imrie, T. Schleeh, F. E. Karasz and G. S. Attard, *Macromolecules*, 1993, **26**, 539-544.
37. E. Nishikawa and H. Finkelmann, *Macromolecular Chemistry and Physics*, 1997, **198**, 2531-2549.
38. G. Galli, E. Chiellini, M. Laus, A. S. Angeloni, O. Francescangeli and B. Yang, *Macromolecules*, 1994, **27**, 303-305.
39. J.-H. Liu and F.-M. Hsieh, *Materials Chemistry and Physics*, 2009, **118**, 506-512.
40. T. Schleeh, C. T. Imrie, D. M. Rice, F. E. Karasz and G. S. Attard, *Journal of Polymer Science Part A: Polymer Chemistry*, 1993, **31**, 1859-1869.
41. Y. Zhao, B. Qi, X. Tong and Y. Zhao, *Macromolecules*, 2008, **41**, 3823-3831.
42. A. Liedtke, M. O'Neill, A. Wertmöller, S. P. Kitney and S. M. Kelly, *Chemistry of Materials*, 2008, **20**, 3579-3586.
43. J.-H. Liu, Y.-L. Chou, R. Balamurugan, K.-H. Tien, W.-T. Chuang and M.-Z. Wu, *Journal of Polymer Science Part A: Polymer Chemistry*, 2011, **49**, 770-780.
44. A. E. Blatch, I. D. Fletcher and G. R. Luckhurst, *Journal of Materials Chemistry*, 1997, **7**, 9-17.
45. H. Khandelwal, A. P. H. J. Schenning and M. G. Debije, *Advanced Energy Materials*, 2017, **7**, 1602209.